Numerical simulation of the dense random packing of a binary mixture of hard spheres: Amorphous metals

A. S. Clarke and J. D. Wiley

Materials Science Program, University of Wisconsin—Madison, Madison, Wisconsin 53703
(Received 3 September 1986)

A new algorithm for the construction of a dense random packing of a binary mixture of hard spheres is presented. The algorithm uses periodic boundary conditions and is capable of handling any binary composition with radius ratio between 1.0 and 2.0. Computed results are relatively insensitive to variations in program parameters. The resulting packings are extremely homogeneous and isotropic. The packing fraction, the radial distribution function, and the Voronoi-cell statistics are all calculated for equal spheres. The packing fraction is also calculated as a function of composition fraction and size ratio for unequal sphere mixtures. For all cases the packing fraction is between 0.64 and 0.68. This contradicts the popular notion that the packing fraction increases rapidly as a function of size ratio for a given composition fraction for dense random packings. Since the mass density scales linearly with packing fraction and amorphous metals have mass densities very close to those of the corresponding crystal, the dense random packing of hard spheres predicts mass densities that are 8—14 % lower than in the crystalline metal. The unlikelihood of this implies that the atoms in an amorphous metal cannot act like hard spheres. Rather they deform in such a way as to pack together more efficiently than a dense random packing of hard spheres.

I. INTRODUCTION

The random close packing of hard spheres model seems to be an excellent approximation to the atomic structure of amorphous metals composed of similar sized atoms (eg. NiP).[1-4] However, most real amorphous metals are binary (or ternary) alloys in which there is a substantial size difference between the smallest and largest atomic radii. It is thought that the size difference raises the stability against crystallization of amorphous metals and also makes it easier to form the amorphous solid (as indicated by lower critical cooling rates, for instance).[5-7] Whether these effects are really due to size differences, chemical bonding effects or a combination of the two is not clear yet.[8] What is clear is that a size difference will substantially change the atomic structure of the amorphous alloy. Consider, for instance, a dense packing of equal spheres in three dimensions. The maximum number of spheres that can touch another sphere is 12.[9] The densest packing of 12 spheres around one is a regular icosahedron (with the atoms at the vertices)[9] (see Fig. 1). However, there is a gap between each outer sphere and its outer neighbors: If the sphere diameter is unity then the minimum distance between outer spheres is approximately 1.05. If we slowly increase the outer sphere diameters we can close the gap, but if there is any further increase the maximum number of outer spheres touching the inner spheres must decrease to 11. Increasing the outer sphere radii further, the number of outer spheres touching the inner sphere must decrease in discrete steps (10,9,...). Similarly decreasing the outer sphere diameter, the maximum number of outer spheres can increase.

Metal-metalloid glasses may exhibit a large degree of chemical short-range order (CSRO). However, metal-metal glasses often exhibit much less CSRO. Because the

dense random packing of a binary mixture of hard spheres does not incorporate any CSRO, it is much more likely to be applicable to metal-metal glasses than metal-metalloid glasses. For a dense random packing of equal spheres the average coordination number (depending on how it is defined) ranges from approximately 12 to 14 with some spheres having as few as 10 neighbors and some as many as 17 [see Fig. 2(a)]. For a dense random packing of unequal spheres some small spheres will be surrounded by only large spheres, some large spheres will be surrounded by only small spheres, and most spheres will have neighbors of each type. Thus we expect a much broader distribution of coordination numbers. We also expect the density (or packing fraction) to increase as we increase the radius ratio; the larger holes being filled by the smaller
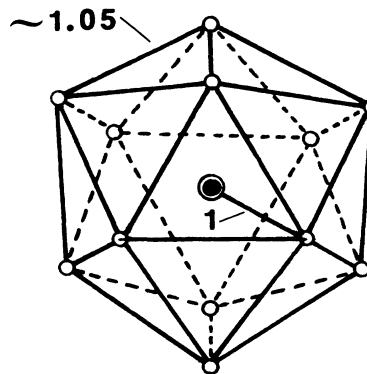
FIG. 1. A regular icosahedron provides the densest packing of 12 atoms around one. If the bond length between the central sphere and all outer spheres is 1.0, then the outer-outer sphere bond length is approximately 1.05.

spheres. In fact this is the basis of the Polk model of metal-metalloid glasses: The small (metalloid) atoms fit into the largest holes in a dense random packing of large (metal) atoms.[10] Since a cluster with small spheres tightly packed around a large sphere is denser than a cluster with large spheres tightly packed around a small one, we might also expect the packing fraction to peak at a high concen-

FIG. 2. Voronoi-cell statistics for a dense random packing of equal spheres constructed using the algorithm described in this paper. (a) Distribution of cells with F faces, (b) distribution of faces with N edges, and (d) distribution of cell volumes.

tration of small spheres. The extent to which these expectations are fulfilled will be addressed in this paper.

There seem to be two types of hard-sphere models of amorphous metals: sequential addition or "cluster" models, and collective rearrangement or "gas compression" models.[11,12] In the sequential addition method a seed of atoms that is incompatible with long-range order (e.g., a tetrahedron or an icosahedron) is chosen. Then atoms are sequentially placed on the "low-energy sites" (in the dimples at the surface of the cluster) using some algorithm. Eventually a large cluster (maybe thousands of atoms) is formed for subsequent structural analysis. In the gas-compression approach N points are placed at random positions within a box. Each point is assigned a radius and the spheres are moved until there are no overlaps. Then the radii are increased and the process is repeated until any further increase in radii or any displacement of the spheres creates overlaps that cannot be eliminated.

There are several problems with models built using sequential addition.[11,12] In at least one case it has been shown that this method produces packings that are not isotropic or homogeneous on any scale up to the size of the model.[13] The authors found significant differences in structure as a function of position and direction in their clusters.[13] The ideal amorphous metal should be isotropic and homogeneous (at least on a scale of $\gtrsim 5-10$ atomic diameters). Models built using sequential addition also have lower packing fractions (from 0.52 to 0.60 depending on the algorithm) than those that are constructed using collective rearrangement.[11,12] This illustrates another problem with this type of modelling: Different algorithms give different structures, as measured by radial distribution functions (RDF's), and packing fraction.

In contrast, collective rearrangement models seem to converge to a unique structure that agrees well with experimental sphere packings.[12,14-17] Several experiments by Scott and Finney (using different methods) produced the same packing fractions ($\eta = 0.6366 \pm 0.0005$). Finney also measured the positions of the spheres in one experiment
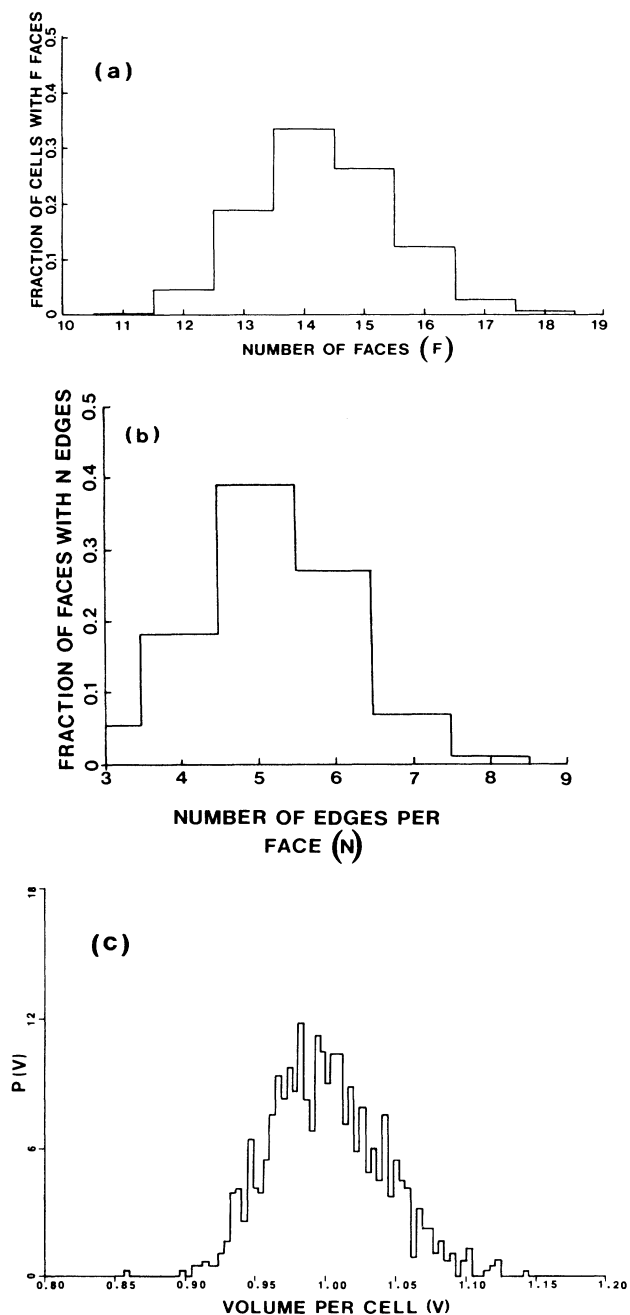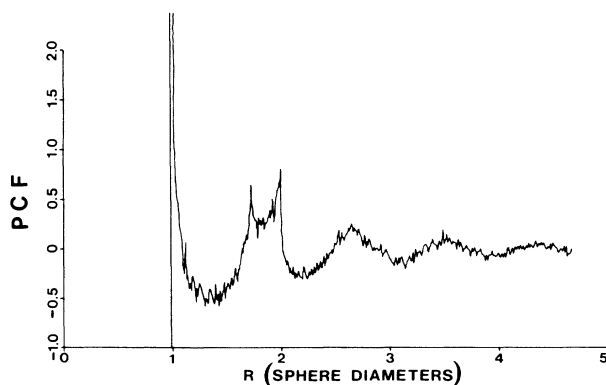
FIG. 3. Pair correlation function (PCF) for a dense random packing of equal spheres constructed using the algorithm described in this paper. The pair correlation function is equal to the radial distribution function minus 1.0.

and from these calculated the Voronoi-cell statistics and RDF's. More recently Jodrey and Tory performed a computer simulation of a dense random packing of equal spheres using cubic periodic boundary conditions and obtained the identical RDF's and packing fractions between 0.637 and 0.649.[16,17] As long as care is taken so that the packing does not "crystallize" at the boundary, all of these laboratory and computer experiments give the same results: homogeneous, isotropic packings with $\eta \approx 0.64$ and Voronoi cell statistics and a pair correlation function (PCF) as in Figs. 2(a), 2(b), 2(c), and 3.

II. THE ALGORITHM

Our algorithm is designed to simulate the dense random packing of a binary mixture of hard spheres. The final configuration is produced using a collective rearrangement algorithm. No chemical short-range ordering effects are incorporated. All previous algorithms (by other authors) either use a sequential addition algorithm combined with chemical short-range ordering rules, or else only consider a dense random packing of equal spheres using collective rearrangement. Thus our algorithm is unique.

The algorithm is based on several very simple ideas. Starting with a random distribution of points inside a box we assign radii to the points to define spheres. In general, the spheres overlap so we must move them to reduce overlaps. If the radii are too large it may not be possible to remove all overlaps by simply moving the spheres, so we must decrease the radii. If the initial radii are too small we may be able to move all the spheres apart so that some spheres are not touching any others; then to reach a high density we must increase the radii. Alternatively, suppose we have an overlap-free packing in which each sphere is touching several others. We have no way of knowing whether this is the highest-density random packing attainable. Therefore we must test this by increasing the radii, moving the spheres to reduce overlaps (then possibly decreasing the radii) until there are no overlaps. Then we compare the resulting overlap-free packing fraction with the previous packing fraction. We repeat this until the overlap-free packing fractions converge. It is possible (though not likely) that the packing may converge to a low-density stable packing (such as a simple cubic lattice). Once the spheres are in such a configuration no amount of increasing or decreasing the radii will change the structure—the spheres are locked into place. To prevent just this kind of occurrence we vibrate the spheres by giving each sphere a small random displacement independent of its neighbors' positions. This unlocks the spheres and allows them to find higher-density configurations.

We can further increase the rate of convergence to the highest packing fractions by moving the spheres as much as possible at each step. This is accomplished by increasing the radii until the maximum overlap is greater than or equal to some tolerance Δ_{toll}. Since the distance each sphere moves is proportional to the magnitude of the overlaps, increasing the size of the allowed overlaps speeds up the program. Increasing the allowed overlap Δ_{toll} also allows the spheres to sample a larger volume at each step, reducing the tendency for spheres to become "locked up." Thus, a large value of Δ_{toll} accelerates the program's rate of convergence and causes it to converge to a higher packing fraction. This trend apparently saturates above $\Delta_{toll} \simeq 0.20$ since the packing fraction never exceeds 0.645 (for equal spheres) under any conditions for $N \gtrsim 100$. A more detailed explanation of the algorithm follows.

Using periodic boundary conditions we place N random points in a cube $0 < x, y, z < 1$. Some number of these points is specified to be small (N_s) and the rest are large (N_l). The radii $(R_s$ and $R_l)$ are determined so that the initial nominal packing fraction is

$$\eta_0 = 4/3\pi R_s^3 N_s + 4/3\pi R_l^3 N_l , \tag{1}$$

where η_0 is between 0 and 1. The initial packing fraction is not the true packing fraction because in general there will be overlaps among the spheres. To reduce the overlaps we then move the spheres one at a time along the vector sum of the overlaps as in Fig. 4.

At low packing fractions most moves will reduce or eliminate overlaps. However, as the packing fraction increases, moving a sphere along the vector sum of the overlaps reduces some overlaps but creates or increases others. To counteract this tendence we accept a move as long as it does not create any overlap as large as the maximum overlap among all the spheres. Thus, the maximum overlap always decreases or stays the same. We found by trial and error that accepting the move only if it reduces the maximum overlap of the sphere being moved is too stringent—the spheres tend to become locked up. If the move is not accepted for a particular sphere the sphere is moved again in the same direction but by a smaller amount. If this is not successful (after a few attempts) the sphere is given a small random displacement. Again, the move is accepted or rejected depending on whether the maximum overlap is less than or greater than the max-
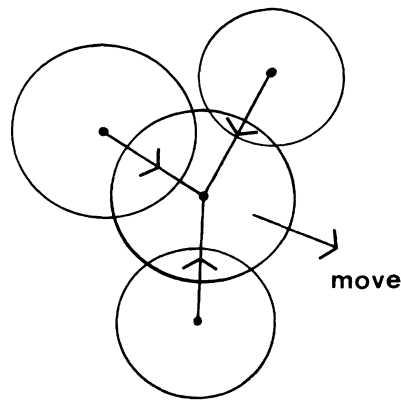
FIG. 4. The central sphere moves along the vector sum of the overlaps. The move is accepted if the new maximum overlap is less than the maximum overlap among all the spheres. This guarantees that the maximum overlap among all spheres will not increase.

imum overlap among all the spheres. Each sphere in the packing $(I = 1, 2, \ldots, N)$ is moved sequentially in this way.

Using this scheme the maximum overlap exhibits a rapid initial decrease. All the spheres are moved in this way until the maximum overlap drops below some tolerance (Δ_{tol1}). Then the radii are increased so that R_l / R_s remains constant. This procedure (move, increase radii) is repeated until finally the maximum overlap does not drop below Δ_{tol1} within some specified number of steps (I_{max}). Then the radii are decreased slowly (each time moving the spheres to reduce overlaps) until the maximum overlap drops below some other (smaller) tolerance (Δ_{tol2}). At this point the packing is almost overlap free so the nominal packing fraction is approximately equal to the true packing fraction. Now we increase the sphere radii again and repeat the whole sequence many times until the packing fractions at the end of each cycle approach a constant value. Then we decrease all tolerances and repeat the procedure several more times to "fine tune" the resulting packing (see Fig. 5).
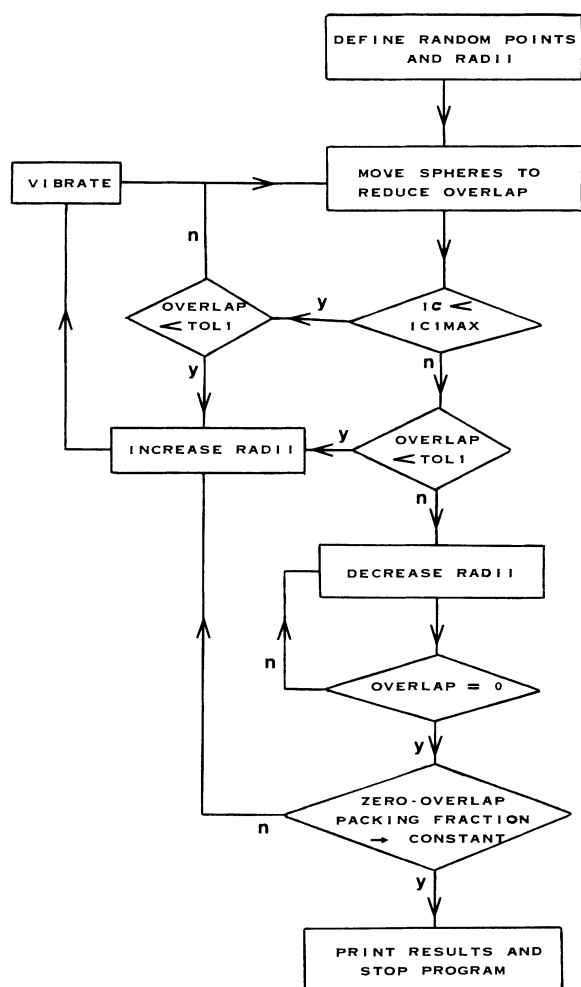
We vibrate the spheres by giving each sphere a small random displacement approximately every other step during the increasing radius phase without regard to whether the overlaps increase or decrease. This greatly improves the rate of convergence of the program since about 90% of the time it takes the program to converge is spent reaching the last 1% or 2% of the final packing fraction. We optimized the parameters (vibration amplitude, vibration frequency, Δ_{tol1}, Δ_{tol2}, etc.) by trial and error to improve the convergence. Then we varied the parameters from the "optimal" values to test the sensitivity of our results. We found that our results are very insensitive to variations in the parameters. The only significant effect is that the program takes longer to converge to the same packing fraction or it converges to a slightly lower packing fraction if the parameters are not close to their optimal values.

The program is capable of handling from approximately 100 to 10 000 spheres with any binary composition fraction and radius ratios between 1.0 and 2.0 A typical 1000 equal-sphere run takes approximately 10 h (CPU time) to converge on an Apollo 460 computer. The program speed scales linearly with the number of spheres because of the method used to calculate overlaps of neighboring spheres. The unit cube is divided into cubic cells with edge length slightly larger than the diameter of the large sphere diameter. Then each sphere I $(I = 1, 2, \ldots, N)$ sits in exactly one cell and all possible overlapping neighbors are contained within the 26 adjacent cells or the cell containing sphere I. These cells are then searched for overlapping spheres. Since only approximately 27 spheres are tested for overlaps for each sphere I, the run time is approximately linear with the total number of spheres.

FIG. 5. Program flow chart. IC is the number of steps since the last time the spheres were increased or decreased.

III. RESULTS

A. Equal spheres

Our results for equal spheres are in excellent agreement with the experimental results of Finney and Scott, and the computer results of Jodrey and Tory. We obtained packing fractions from 0.637 and 0.645 for equal spheres depending on sample size, duration of the "anneal" (run time), and the values of the program convergence parameters. The packing fraction never exceeded 0.645 for $N \gtrsim 100$. Voronoi cell statistics are shown in Figs. 2(a), 2(b), 2(c) and the pair correlation function is shown in Fig. 3. (The PCF is the RDF) minus one. The PCF exhibits a split second peak with the second subpeak higher than the first subpeak. These features are in common with all the previous authors results. The packing is homogeneous to a very small scale as can be seen from Table I. It is also isotropic (angular correlations in these sphere packings will be discussed in a future paper). We find no regions of crystallization as can be seen from Figs. 2(c) and 3 and Table I. If there were any crystallization we would expect at least one of the following: a sharp peak (or peaks) in the low volume end of the Voronoi cell volume distribution, a sharp peak (or peaks) in the PCF, or high-density clustering in Table I. We see none of these. Thus the cubic periodic boundary conditions do

TABLE I. We divide the cube into 27 and 8 cells, respectively and tabulate the number of sphere centers in each cell. Entries below are the numbers of sphere centers found in each cell.

27 CELLS

```
         39   34   34
         38   40   37
         36   39   38
    32  40   38
    37  36   34
    37  41   39                      8 CELLS
36  37  39                      122   123
39  39  34                        130   124
37  35  35                   127   123
                             126   125
```

FIG. 6. Packing fraction as a function of size ratio and composition fraction for dense random packings of hard spheres. The dashed line indicates the experimental result obtained by Finney and Scott for equal spheres.

not induce crystallization in any of these runs. It is also worth noting that all of our results (pair correlation functions, Voronoi cell statistics, etc.) are extremely insensitive to sample size for $N \geq 100$.

B. Unequal spheres

A much more detailed presentation of the unequal sphere results will be given in a future paper. Here we just give some highlights.

We varied both radius ratio and composition fraction over a wide range to study the associated changes in packing fraction and structure (see Table II). Packing fraction as a function of size ratio and composition fraction is shown in Fig. 6. As discussed in the Introduction, we expect the packing fraction to increase with increasing R_l/R_s for fixed composition fraction. For fixed R_l/R_s, we expect the maximum packing fraction to be at a high concentration of small spheres. Both expectations are fulfilled but the magnitude of the changes is surprisingly small. Between $R_l/R_s = 1.0$ and 1.3 the packing fraction is approximately constant, independent of composition. Even for $R_l/R_s = 2.0$ the highest packing fraction is only ≈ 0.68, whereas $\eta = \pi/\sqrt{18} = 0.740\ldots$ for close-packed crystalline arrays of equal spheres.

A comparison of our computer results with curve fits to the experimental results obtained by Yerazunis, Cornell, and Wintner[18] is shown in Fig. 7. Here y is the ratio of the volume occupied by large spheres divided by the volume occupied by all spheres,

$$y = \frac{N_l v_l}{N_s v_s + N_l v_l}, \qquad (2)$$

where $v_{l(s)}$ is the volume of a large (small) sphere. Our results follow the same trends as their data. As $R_l/R_s \to \infty$ the dense random packing becomes a dense random packing of large spheres with a dense random packing of small spheres occupying the interstices. Thus the packing fraction (at $R_l/R_s \to \infty$) has a maximum of $\approx 0.64 + 0.64 \times (1.0 - 0.64) \approx 0.87$ at $y \approx 0.64/0.87 \approx 0.73$. The authors in Ref. 18 model this situation using a "distortion parameter" formulation in which small spheres pack into the interstices of the large sphere packing more and more efficiently as $R_l/R_s \to \infty$. However, as R_l/R_s decreases toward 1.0 this picture becomes more and more incorrect. Our results for low R_l/R_s show the correct behavior: The maximum packing fraction drops rapidly to the equal sphere value as $R_l/R_s \to 1.0$ and the peak position shifts to the left. Below $R_l/R_s \approx 2$ the effect of mixing small and large spheres in a dense random packing becomes much more complicated because the presence of each type of sphere strongly affects the arrangement of the other type of spheres.

TABLE II. Dense random packings were constructed with all 35 combinations of the below composition fractions and size ratios using the algorithm described in this paper.

	Percent small spheres				
	20	40	60	80	90

	Size ratio (R_l/R_s)					
1.1	1.2	1.3	1.4	1.5	1.75	2.0
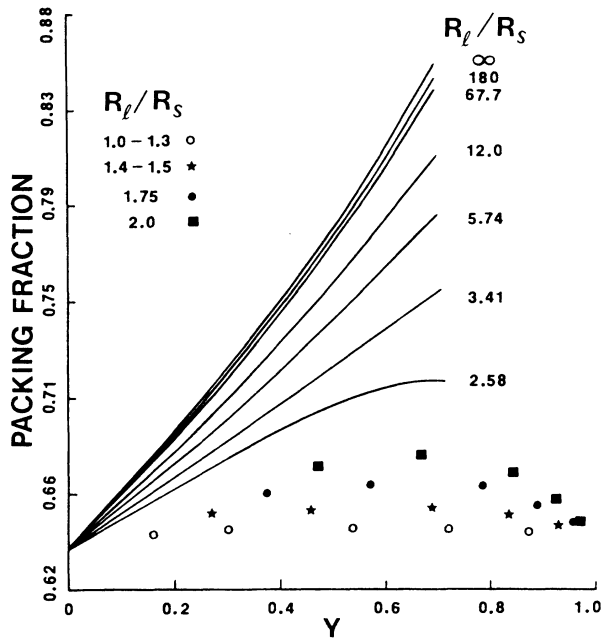
FIG. 7. Packing fraction as a function of size ratio and composition fraction for dense random packings of hard spheres. Solid lines are the curve fits to the experimental results obtained by Yerazunis, Cornell, and Wintner (Ref. 18). Our numerical results are plotted using symbols. Y is defined in the text.

C. Mass density versus packing fraction

The packing fraction η is related to the mass density ρ for a binary mixture of hard spheres by

$$\rho = \frac{N_s m_s + N_l m_l}{N_s v_s + N_l v_l} \eta \ , \tag{3}$$

where $m_{l(s)}$ is the mass per large (small) sphere. We denote the crystalline state by subscript c, the amorphous state by subscript a, and define $\Delta\eta = \eta_c - \eta_a$ and $\Delta\rho = \rho_c - \rho_a$. We then obtain

$$\frac{\Delta\rho}{\rho_c} = \frac{\Delta\eta}{\eta_c} \ . \tag{4}$$

Assume, for the moment, that an amorphous metal has the structure of a dense random packing of hard spheres and that the atoms have the same effective hard sphere radius in the glass as they do in the crystal. If the crystal is close packed then it will have a packing fraction of approximately 0.74. The dense random packing of hard spheres has a packing fraction of between 0.64 and 0.68 for all compositions and radius ratios up to 2:1. Thus the mass density of the amorphous metal must be from $(0.74-0.68)/0.74 \approx 8\%$ to $(0.74-0.64)/0.74 \approx 13.5\%$ lower than the mass density of the corresponding crystal. However, real amorphous metals typically are only 0.5—2 % less dense than the corresponding crystal. Since ρ is inversely proportional to sphere volume [Eq. (3)] and volume is proportional to the radius cubed, the only way

the discrepancy between the crystalline and amorphous mass densities can be reconciled (for hard spheres) is for the effective hard-sphere radius to be $\sim 3\%$ to 5% lower in the amorphous metal than in the crystal. However, the average coordination number in amorphous metals is very close to the average coordination number in the crystal.[2] The effective radius depends mainly on coordination number (assuming similar chemical environments) and a decrease from 12 to 8 in coordination number corresponds roughly only to a 3% decrease in radius.[19] It therefore appears that the hard-sphere model must be viewed as only a relatively crude approximation to the behavior of atoms in amorphous metals. In reality, the atoms appear to deform in such a way as to fill space more efficiently than a dense random packing of hard spheres.

IV. SUMMARY AND CONCLUSIONS

We have simulated the atomic structure of amorphous metals using a program that constructs a dense random packing of a binary mixture of spheres of arbitrary composition fraction and radius ratio between 1.0 and 2.0. The algorithm uses periodic cubic boundary conditions and moves the spheres along the vector sum of their overlaps. Vibration of the spheres greatly increases the rate of convergence to a high density, overlap-free packing. Our results are identical to other authors' for equal spheres and are very insensitive to variations in the values of the parameters used in the program. This supports our belief that dense random packings of spheres are nearly independent of the algorithm (or method, in the case of laboratory measurements) used to construct them.

For unequal spheres the packing fraction increases only slightly with increasing size ratio. The maximum packing fraction always occurs at a high concentration of small spheres. We find the surprising result that the packing fraction is approximately constant for all composition fractions and radius ratios between 1.0 and 2.0. Since the mass density scales linearly with the packing fraction the dense random packing of the hard-spheres model predicts that amorphous metals are 8% to 14% less dense than real amorphous metals. For a hard-sphere model this can only be reconciled by reducing the effective hard-sphere radii by 3% to 5% from the crystal to the amorphous metal. However, the average coordination number is approximately the same in the crystal and amorphous phases. Since effective atomic radii depend mainly on the coordination number (for similar chemical environments) it is extremely unlikely that the radii uniformly decrease by as much as even 3%. Rather, the atoms in amorphous metals act more like frogs' eggs or caviar—they are not spherical.[20] This sponginess allows the atoms to pack more efficiently than would be possible if they acted like hard spheres. The deviation of the atomic radii needed to reconcile the discrepancy between the observed mass density and the mass density predicted by the dense random packing of hard spheres is at least 3%. This applies a fortiori to other hard-sphere models of amorphous metals because the discrepancy between the observed and predicted mass densities is even greater.

[1]G. S. Cargill III, J. Appl. Phys. **41**, 12 (1970).
[2]R. Zallen, *The Physics of Amorphous Solids* (Wiley, New York, 1983).
[3]P. K. Leung and J. G. Wright, Philos. Mag. **30**, 185 (1974).
[4]P. K. Leung and J. G. Wright, Philos. Mag. **30**, 995 (1974).
[5]S. Mader, Thin Solid Films **35**, 195 (1976).
[6]I. W. Donald and H. A. Davies, J. Non-Cryst. Solids **30**, 77 (1978).
[7]M. M. Collver and R. H. Hammond, J. Appl. Phys. **49**, 2420 (1978).
[8]H. S. Chen and B. K. Park, Acta Metall. **21**, 395 (1973).
[9]L. Fejes Toth, *Regular Figures* (Pergamon, New York, 1964), pp. 292–300.
[10]D. E. Polk, Scr. Metall. **4**, 117 (1970).
[11]M. R. Hoare, J. Non-Cryst. Solids **31**, 157 (1978).

[12]J. L. Finney, in *Amorphous Metallic Alloys,* edited by F. E. Luborsky (Butterworths, London, 1984).
[13]D. S. Boudreaux and J. M. Gregor, J. Appl. Phys. **48**, 152 (1977).
[14]J. L. Finney, Ph.D. thesis, Birkbeck College, London, 1968.
[15]G. D. Scott, Nature **188**, 908 (1960).
[16]W. S. Jodrey and E. M. Tory, Phys. Rev. A **32**, 2347 (1985).
[17]W. S. Jodrey, E. M. Tory, J. Powder Technol. **30**, 111 (1981).
[18]S. Yerazunis, S. W. Cornell, and B. Wintner, Nature **4999**, 835 (1965).
[19]W. Hume-Rothery, R. E. Smallman, and C. W. Haworth, *The Structure of Metals and Alloys* (The Metals and Metallurgy Trust, London, 1969), pp. 71–109.
[20]D. R. Nelson, Phys. Rev. B **28**, 6377 (1983).